Published in final edited form as:
Gene Expr Patterns. 2013 January ; 13(1-2): 21–29. doi:10.1016/j.gep.2012.09.001.

Immunohistochemical analysis of sphingosine phosphate lyase expression during murine development

Susan Newbigging[a], **Meng Zhang**[b], and **Julie Saba**[b,*]

[a]Centre for Modeling Human Disease, Samuel Lunenfeld Research Institute, Mount Sinai Hospital; and Physiology and Experimental Medicine Research Program, The Hospital for Sick Children, both at The Toronto Centre for Phenogenomics, and the University of Toronto, Toronto, Ontario, Canada

[b]Children's Hospital Oakland Research Institute, Oakland, CA 94609, USA

Abstract

Sphingosine-1-phosphate lyase (SPL) catalyzes the degradation of sphingosine-1-phosphate (S1P), a bioactive lipid that controls cell proliferation, migration and survival. Mice lacking SPL expression exhibit developmental abnormalities, runting and death during the perinatal period, suggesting that SPL plays a role in mammalian development and adaptation to extrauterine life. We investigated the pattern of SPL expression in the mouse embryo and placenta from day 8 to day 18. Our findings reveal that SPL is expressed in the developing brain and neural tube, Rathke's pouch, first brachial arch, third brachial arch, optic stalk, midgut loops, and lung buds. Diffuse signal was high at E12, whereas a recognizable adult SPL pattern was evident by E15 and more intensely at E18, with strong expression in skin, nasal epithelium, intestinal epithelium, cartilage, thymus and pituitary gland. These findings suggest SPL may be involved in development of the mammalian central nervous system (CNS), anterior pituitary, trigeminal nerve, palate and facial bones, thymus and other organs. Our findings are consistent with the SPL expression pattern of the adult mouse and with congenital abnormalities observed in SPL mutant mice.

Keywords

sphingosine-1-phosphate; sphingosine phosphate lyase; S1P lyase; *Sgpl1*; embryogenesis; sphingolipid

1. Introduction

Sphingosine-1-phosphate lyase (SPL; EC 4.1.2.27, or sphingosine-1-phosphate aldolase) catalyzes the irreversible degradation of sphingosine-1-phosphate (S1P), a lipid signaling molecule which has been implicated in diverse developmental and physiological functions including cell proliferation, migration, programmed cell death, inflammation, hematopoietic cell trafficking and angiogenesis (Maceyka et al., 2012). SPL is a highly conserved integral

*Corresponding author: Julie D. Saba, Children's Hospital Oakland Research Institute, 5700 Martin Luther King Jr. Way, Oakland, CA 94609-1673, USA. Tel.: +1 510 450 7690; fax: +1 510 450 7910, jsaba@chori.org (J. Saba).

membrane protein located in the endoplasmic reticulum (ER) in all species in which it has been characterized (Serra and Saba, 2010). Loss of SPL expression leads to significant increases in tissue and plasma S1P levels, and SPL is also responsible for maintaining the steady state levels of S1P inside the cell. (Bektas et al., 2010; Siow et al., 2010). By serving as the primary regulator of cellular and tissue S1P levels, SPL controls S1P pools available for intracellular signaling as well as for export and extracellular signaling through G protein-coupled S1P receptors (S1PRs). SPL cleaves S1P at carbon bond C2-3, resulting in the formation of ethanolamine phosphate and hexadecenal. The majority of SPL's role in mammalian biology likely results from its influence over S1P signaling. However, some of its functions may be linked to the hexadecenal reaction product, which is a reactive aldehyde. Hexadecenal has been shown to participate in c-Jun Kinase-mediated cell signaling, apoptosis, adhesion, can form adducts with DNA, and serves as a substrate for fatty aldehyde dehydrogenase, the latter which is deficient in patients with Sjögren-Larsson syndrome (Kumar et al., 2011; Nakahara et al., 2012; Upadhyaya et al., 2012). Importantly, SPL catalyzes the only exit path for sphingolipid removal, represented by the final biochemical step in sphingolipid catabolism in which S1P is converted to metabolites that are used in phospholipid biosynthesis. As such, SPL also exerts control over the entire sphingolipid metabolic pathway, and its inhibition results in accumulation of sphingolipid intermediates (Vogel et al., 2009).

In mammals, SPL is expressed in most cells except for blood erythrocytes and platelets, although the relative amount of SPL varies considerably depending upon the organ, tissue substructure and cell type (Borowsky et al., 2012). SPL is encoded by the *Sgpl1* gene in mice and in humans (Van Veldhoven et al., 2000; Zhou and Saba, 1998). No human disease has yet been attributed to loss of SPL function or mutation of human *Sgpl1*. However, mutant mice lacking SPL expression due to targeted disruption of *Sgpl1* exhibit anemia, a variety of developmental abnormalities, runting and do not live beyond the weaning period (Allende et al., 2011; Bektas et al., 2010; Schmahl et al., 2007; Vogel et al., 2009).

A number of genetic abnormalities have been observed in SPL knockout mice. Schmahl and colleagues identified the murine *Sgpl1* gene in a gene trap–coupled microarray approach used to identify intermediate early genes regulated by PDGF (Schmahl et al., 2007). They then generated *Sgpl1* null mice and demonstrated that, like other PDGF target genes identified in their screen, *Sgpl1* mutants exhibit phenotypes similar to PDGF mutants, including anemia and defects in kidney and vasculature, as well as abnormalities of bone and bone marrow derived cells of the myeloid lineage (Schmahl et al., 2007). Additional studies performed by another research group on this knockout line revealed abnormalities of lipid storage, innate immune cell trafficking and cytokine regulation (Bektas et al., 2010) (Allende et al., 2011). *Sgpl1* knockout mice were generated independently by Lexicon, and similar phenotypes as well as additional abnormalities were identified, including lung disease and lesions of the heart, urinary tract, and bone (Vogel et al., 2009). Specifically, these mutant mice were found to exhibit alveolar proteinosis, osteopetrosis, cardiomyopathy and urothelial vacuolization. In the current study, we show that SPL is expressed early in the developing bone, cartilage, bladder, heart and lung, as well as in cytokine-producing epithelial cells of the gut and lung mucosa. Together, these findings strongly suggest that SPL exerts important functions in the developing embryo that are necessary for proper organ development, establishment of innate and adaptive immune systems and mucosal integrity. In addition, the immune system of SPL knockout mice are severely affected, with peripheral lymphopenia, elevated circulating neutrophil and monocyte counts, depletion of thymic cortical lymphocytes with increased cellularity in the thymic medulla and other features consistent with a block in the egress of mature T cells from the thymus (Vogel et al., 2009; Weber et al., 2009). These findings are consistent with the known function of SPL, S1P and $S1P_1$ in regulating lymphocyte trafficking and suggest that SPL plays a much broader role in

mammalian development and adaptation to extrauterine life (Matloubian et al., 2004; Schwab et al., 2005).

Despite the significant impact that loss of SPL exerts on murine development and early post-natal life, the ontogeny of SPL expression throughout mammalian development has not been examined in depth. We recently evaluated SPL expression in the E17 mouse embryo, which exhibited a pattern similar to that of the adult mouse (Borowsky et al., 2012). However, we suspected that investigation of earlier stages might reveal more interesting findings about SPL's potential role in development. We therefore investigated the pattern of SPL gene expression in the mouse embryo at four stages of development from day 8 to day 18. In addition, we have characterized the spatial expression pattern of murine SPL in early placental tissues. Our findings are novel and illustrate that SPL is likely to play important roles in prenatal development. Specifically, we interpret our findings to suggest that SPL may have: 1) embryonic functions that help to prepare the organism for extrauterine life, 2) embryonic functions of a specifically developmental nature, and 3) placental functions that may support fetomaternal exchange.

2. Results

2.1 Temporal SPL expression in mouse embryos

For wild type embryos at E12, there is ubiquitous immunopositivity throughout the tissue section (Figure 1A). At E15, there also is ubiquitous expression across all organ systems in the embryo, although the signal level is decreased a level in intensity compared to the E12 wild type embryos (Figure 1B). By E18, compared to the early time points examined, there is more tissue-specific and localized positive immunostaining (Figure 1C), as described in the sections that follow. For all positive cell types, there is no signal observed within nuclei, and signal is restricted to the cytoplasm. For all *Sgpl1* null tissue sections, no signal is detected in any cell type, as shown in Figures 1D–E.

2.2 SPL expression in trophoectoderm

Placental sections from time point E8 were immunostained and microscopically evaluated. Within the decidual layer, trophoblasts are diffusely stained with moderate to strong cytoplasmic signal (Figure 2A). The pattern of positive signal is coarsely stippled to vacuolated in appearance, located in the perinuclear region and extending toward the plasma membrane (Figure 2B). Further into the central region of the placenta, trophoblast giant cells show minimal to no signal in the cytoplasm (Figure 2C). Within the spongiotrophoblast layer, the cytoplasmic signal ranges from minimal to mild, with the majority of the cells having mild staining. Spongiotrophoblasts within the labyrinth layer exhibit signal that is weaker compared to that observed in spongiotrophoblasts in the decidual layer (Figure 2D).

2.3 SPL expression in ectoderm

At E8 the cells of the neural fold show mild to moderate positive cytoplasmic signal (Figure 3D). By E12, cells lining the telencephalic and mesencephalic vesicles (Figure 3A), third and fourth ventricles (Figure 3A), neuroepithelium of the neural tube (Figure 3D), Rathke's pouch (Figure 3B), mandibular component of the first brachial arch (Figure 3C), third brachial arch (data not shown), optic stalk (data not shown) all have strong positive cytoplasmic staining. At E15 there is strong intensity of immunohistochemical signal in the neopallial cortex (data not shown), choroid plexus (Figure 3E), retina (data not shown), mesencephalon (Figure 1B), lateral ventricles (Figure 1B), fourth ventricle (data not shown), presumptive trigeminal ganglion (data not shown), and dorsal root ganglion (Figure 3G). Concomitantly at E15, the majority of the olfactory epithelium exhibits generalized mild cytoplasmic staining (Figure 3F) as well as a few multifocally scattered cells that display a

strong, vacuolated cytoplasmic signal (Figure 3F). At E18 there is a strong signal in nasal epithelium (Figure 3J) and mild signal along the spinal cord (Figure 3I).

In the developing integument system, by E12 the majority of the positive staining appears to be cytoplasmic and strongest in the epidermis (Figure 3D), and this continues at E15, where the strongest signal of all tissues is in the epidermis (Figure 3H). At E18, the strong signal in the skin continues to be evident (Figure 3K), including the developing pilosebaceous unit (Figure 3L).

2.4 SPL expression in mesoderm

Sections from E8 yolk sac and amnion were examined microscopically. The parietal and visceral layers of the yolk sac show moderate intensity of positive cytoplasmic signal in all of the columnar epithelial cells that make up this membrane (Figures 4A and C). The blood island endothelial cells exhibit minimal to moderate positive cytoplasmic signal (Figures 4B), while precursor *fetal* red blood cells (proerythroblasts, erythroblasts, and normoblasts), produced by and housed within the blood island, have minimal positive cytoplasmic signal. The amniotic cells reveal a moderately positive cytoplasmic signal (Figure 4A). Within the labyrinth layer of the placenta, maternal endothelial cells contain faint to weak cytoplasmic signal, and mature red blood cells within these maternal vessels are negative (Figure 2C). All mature red blood cells in all areas of the placenta are devoid of immunohistochemical signal. In contrast to the positive signal in fetal endothelium, endothelial cells within all placental blood vessels exhibit minimal or no cytoplasmic signal.

At E12 there is no staining in hematoblasts that fill vascular channels, heart chambers (Figure 4D) or liver sinusoids. Sections from E15 and E18 embryos reveal no signal in mature red blood cells (Figure 4E and F). The cardiovascular system including myocytes, endocardium, epicardium, pericardium and all endothelium throughout the fetus exhibit mild to moderate positive cytoplasmic staining at E12 and E15 (Figures 4D and E). By E18 the intensity of the cytoplasmic signal in the aforementioned cardiovascular cells is minimal to mild (Figure 4F).

Lymphocytes in the thymus at E15 show minimal intensity of cytoplasmic signal (Figure 4H), whereas at E18 they do not have any immunohistochemical signal (Figure 4I).

Chondrocytes have mild to moderate cytoplasmic staining at E15. However, by E18 there is a notable decrease in intensity ranging from minimal to mild (Data not shown).

2.5 SPL expression in endoderm

At E12 midgut loops show a strong cytoplasmic signal, as do the lung buds (Figures 5A–C). At E15 all of the future mucosal lining throughout the developing small and large intestine have mild cytoplasmic staining (Figure 5F), while the three outer layers –future submucosa, muscularis mucosa, and serosa (Figure 5E) — as well as the primordial pancreas, exhibit minimal to mild cytoplasmic staining. At E18, the signal decreases throughout the outer three layers to minimal (Figure 5H), while the signal in the mucosa stays mild throughout the cytoplasm of the enterocytes (Figure 5I). However, there is an increase to moderate intensity at the apical portion of the enterocyte's cytoplasm (Figure 5I). In the developing respiratory system at E15, immunostaining reveals the primordial bronchiolar epithelium, alveolar epithelium and pleura all show a moderate to strong cytoplasmic signal (Figure 5D). However, by E18, there is a complete absence of signal in all lung tissue (Figure 5G).

Cells in the E12 and E15 primordial liver consist of a mixture of red blood cell precursors that are immunohistochemically negative for SPL signal while primordial hepatic cells have

a range of minimal to strong cytoplasmic positive signal (data not shown). By E18, the cytoplasmic signal is at best minimal in the hepatic cells (Figure 1C).

Thyroid gland was only visible in sections at time point of E18 and shows minimal cytoplasmic signal in developing follicular cells (data not shown).

The primordial thymus exhibits mild positive signal at E12 (Figure 4G). Thymus epithelium at E15 is positive in patchy areas throughout the organ with mild to strong positive cytoplasmic staining in reticular cells (Figure 4H), evident at E18 as well (Figure 4I).

3. Discussion

In this study, we have characterized SPL expression from E8 to E18 of the developing mouse and associated placental tissues and yolk sac by performing immunohistochemical analysis of wild type mice and corresponding SPL null embryos. The staining results using our detection system are highly specific, as demonstrated by a complete absence of staining in the null mouse embryonic tissues. Our results show SPL to be a cytoplasmic protein in all tissues wherein signal could be detected, consistent with its known subcellular localization as an integral membrane protein of the ER. Although in most cells the SPL cytoplasmic staining did not suggest a specific subcellular localization, occasional cells in the olfactory epithelium exhibited a vacuolated pattern, which suggests the enzyme may be compartmentalized differently and have a unique function in this location.

Overall, our results reveal dynamic changes in embryonic SPL expression over time, with strong and diffuse expression observed in many embryonic structures at E12, followed by a general reduction in intensity at E15, and finally developing discrete expression patterns in an organ-specific manner by E18. The finding of strong early expression levels followed by a reduction in expression intensity is consistent with the findings of Fang et al, who characterized the transcriptome of early organogenesis in humans (Fang et al., 2010). In their study, they showed that genes related to glycosphingolipid metabolism fell into a functional cluster involved in cellular metabolism and homeostasis and characterized by high levels of early embryonic expression that waned over time. They postulated that this cluster represented genes with functions involved in “stemness,” stem cell survival, and the initiation of organogenesis. Interestingly, another phenotype associated with this developmental gene cluster was the abnormal circulation of lipids, consistent with the function of SPL as a regulator of the circulating lipid, S1P (Fang et al., 2010). They compared their findings to a transcriptome analysis of murine organogenesis and found that the murine homologs showed similar temporal expression patterns during murine development (Fang et al., 2010; Mitiku and Baker, 2007).

Although the general intensity of SPL expression decreases from E12 to E15, the expression continues to change over time and eventually assumes the tissue-specific SPL expression pattern of the adult mouse. Some patterns of SPL expression in the developing embryo correspond with the characteristic SPL expression patterns of adult tissues, such as positive expression in brain, thymus and intestines and negative expression in mature erythrocytes of the erythroid lineage. For example, organs derived from the telencephalon including the cerebral cortex, basal nuclei, the limbic system and lateral ventricles were positive for SPL expression in this study, as were areas of the mesencephalon, which leads to development of cerebral base and aqueducts. These findings positively correlate with the presence of SPL in adult mouse cerebral cortex, choroid plexus, arachnoid lining cells, midbrain, hindbrain and cerebellum (Borowsky et al., 2012). Rathke’s pouch is the precursor tissue to the anterior and intermediate lobes of the pituitary gland, which exhibited positive SPL signal in the embryo. This also seems to persist throughout adulthood in the mouse, as strong SPL positive signal was also observed in the adenohypophysis (Borowsky et al., 2012). The first

brachial arch leads to development of masticatory muscles, mandibular nerve, and eventually to the bones of the maxilla and mandible. SPL was positive in this arch and correlates with the mouse adult finding of scattered strong expression in the trigeminal ganglion cells (Borowsky et al., 2012). The reason for SPL's high expression in specific areas of the brain is not known. However, neurons that robustly express SPL have been shown to be the first to degenerate in SPL null mice, suggesting that they play a role in maintaining low S1P levels for neuronal survival (Hagen et al., 2011). Specifically, SPL expression is required in order to prevent S1P-induced apoptosis in hippocampal neurons. In contrast, sphingosine kinases (thereby implying S1P biosynthesis) is essential for normal brain development (Hagen et al., 2011; Hagen et al., 2009; Mizugishi et al., 2005). The cumulative results from these studies suggest that the mammalian brain requires tight regulation of S1P levels in the developing and postnatal brain.

The adult mouse thymus exhibits a strong signal in epithelial cells and low signal in lymphocytes (Borowsky et al., 2012). This is consistent with the pattern we observed in mouse embryos, suggesting that SPL may play a critical development role in thymic epithelial functions during embryogenesis and progressing into adulthood. In the developing mouse, the thymus reaches adult size at approximately E14 to E15 (Ward et al., 1999). Further, it is known that during murine development, blood-borne thymocyte precursors derived from hematopoietic stem cells first colonize the primordial thymus at E11.5, prior to vascularization of the tissue (Stein and Nombela-Arrieta, 2005). SPL knockout mice exhibit a block in thymocyte egress, elevation of ceramide levels and thymic atrophy (Weber et al., 2009). It was suggested that SPL deficiency inhibited early thymocytopoiesis by preventing settling of early thymocyte precursors and thereby causing a reduction of early T progenitors in the thymic cortex starting at 2 wk after birth, whereas in contrast the mature thymocytes accumulated in the medulla due to the block in egress. Our findings suggest that SPL expression in the stromal epithelial cells of the developing thymus may play a role in thymocyte homing, differentiation, survival or maintenance of the blood-thymus barrier during prenatal development.

The midgut loops had strong SPL expression at E12, which continued at E15 in the developing intestinal walls with maintained moderate signal throughout the apical cytoplasm of enterocytes. Previous studies have revealed strong expression of SPL in adult intestinal epithelium (Borowsky et al., 2012; Oskouian et al., 2006). SPL is required for metabolism of dietary sphingolipids such as are found in milk, consistent with the high SPL expression localized at the apical cytoplasm in the near term embryo (Duan and Nilsson, 2009).

In contrast to these positive findings, the lack of staining in mature maternal erythrocytes in the placenta and mature erythrocytes throughout mouse embryonic development is consistent with erythrocytes having no detectible SPL and serving as the main source of circulating S1P via uptake and storage of S1P (Hanel et al., 2007).

Interestingly, in some cases SPL expression is detected at moderate levels in embryonic tissues corresponding to structures that exhibit minimal or no detectible SPL expression postnatally. Adult murine heart exhibits minimal SPL expression, although a small amount of expression can be detected in the endocardium of the valves and in cardiomyocytes (Bandhuvula et al., 2011). The mild to moderate signal we observed in the heart tissue at E12 through to E15 had decreased by E18. Our finding that SPL is expressed at higher levels in the early embryonic heart compared to late embryonic and adult hearts suggests that SPL may play an important role in modulation of S1P during embryogenesis. This notion is consistent with striking findings in zebrafish, wherein S1PR mutants exhibit *cardia bifida* due to an S1P signaling requirement during cardiac development. In this process, S1P signaling promotes cell migration toward the midline and thereby fosters fusion of the two

separate heart tubes into one heart structure (Kupperman et al., 2000). Our observations are also consistent with the recent finding that S1P signaling through S1PR1 contributes to the development of the mammalian heart (Poulsen et al., 2011). We propose that cell migrations essential for organogenesis may require S1P gradients regulated by SPL, consistent with the finding that SPL regulates mouse embryonic fibroblast migration *in vitro* (Schmahl et al., 2007). In addition, SPL knockout pups sometimes exhibit evidence of cardiomyopathy, which suggests that cardiomyocyte survival or proliferation in the neonatal heart may be influenced by SPL expression (Vogel et al., 2009).

This is the first study to evaluate the expression of SPL in murine trophoectoderm. It was previously reported that S1P inhibits differentiation of human cytotrophoblasts into syncytiotrophoblasts (precursors to syncytial or giant cells) in cell culture (Johnstone et al., 2005). This notion is compatible with our findings of minimal to mild expression of SPL in the trophoblasts of the decidual layer, and scarce expression in the giant cells, since it is assumed that S1P levels would be low in the latter and, thus, there would not be a need for S1P degradation. A more detailed analysis using confocal microscopy may be required to accurately determine whether the subcellular compartment of SPL expression is unique in this tissue.

Other studies have revealed that the levels of sphingosine kinase 1, which is the main enzyme responsible for producing S1P, rise with increasing gestational age in human decidua. This rise was accompanied by a rise in SPL expression (Yamamoto et al., 2010). Our murine study reveals a comparable pattern of expression at E8. S1P signaling is critical for vascular maturation in the embryo and for maintaining vascular integrity and preventing vascular leak postnatally (Liu et al., 2000; Olivera et al., 2010; Peng et al., 2004). Throughout the decidua and mainly in the labyrinth, fetal capillaries are surrounded by a thin layer of connective tissue followed by enveloping trophoblasts (Watson and Cross, 2005). The maternal blood bathes this region and thus is a major area of maternal-fetal exchange of nutrients (Adamson et al., 2002). This complex arrangement between the vasculature and trophoblast requires interactions between the different cells, including rearrangement of fibroblasts for vasculogenesis and angiogenesis (Adamson et al., 2002).

3.1 Conclusions

Our findings reveal that SPL is expressed in the developing brain and neural tube, developmental structures including Rathke's pouch, mandibular component of the first brachial arch, third brachial arch, optic stalk, midgut loops, and lung buds. Diffuse, strong expression was characteristic of early developmental stages, followed by diminished expression intensity at midgestation, and a recognizable adult SPL pattern emerged prior to birth with strong expression in skin, nasal epithelium, intestinal epithelium, cartilage, thymus and pituitary gland. These findings implicate SPL function in the development of the mammalian CNS, anterior pituitary, trigeminal nerve, palate and facial bones, thymus and other organs. Our findings are consistent with adult SPL expression pattern and with the developmental abnormalities that have been observed in SPL mutant mice. However, our findings also suggest that SPL may serve strictly developmental functions in some organs.

4. Experimental procedures

4.1 Mouse husbandry

Mice harboring the *Sgpl1* null allele were derived by gene trap mutagenesis as previously described (Schmahl et al., 2007). The line was generously provided by Philippe Soriano, Mount Sinai School of Medicine, New York, NY. The mice were originally on a mixed C57BL6/129sv background. They were subsequently backcrossed more than six times and have been maintained in this C57BL/6 background by heterozygous matings and used to

generate the wild type and knockout progeny used in this study. Animals were maintained in the Children's Hospital Oakland Research Institute (CHORI) AAALAC Accredited Animal Facility. All experiments were conducted in accordance with CHORI Institutional Animal Care and Use Committee approved protocols.

4.2 Embryo isolation

Embryos were removed from the uterus and yolk sac of pregnant mice at various days of gestation as described (Nagy et al., 2003). Genotyping was performed to identify knockout embryos that were employed as negative controls for immunohistochemical staining. Representative parasagittal sections of day 8 placenta and of day 8, 12, 15 and 18 embryos were stained for SPL as described below.

4.3 Genotyping

Mouse embryos were genotyped, and mice homozygous for the wild type allele were used to establish normal SPL expression pattern during embryogenesis, with homozygous null mice serving as negative controls. Mouse embryo sections were used for genotyping. Embryos were dissected and immersed immediately into fresh phosphate-buffered saline (PBS) containing 4% paraformaldehyde. After fixation for 24 hours at 4°C, samples were washed in PBS, dehydrated through a graded series of ethanol washes, cleared in xylenes, and embedded in paraffin. Sections were cut at a thickness of 5 microns and mounted onto slides treated for adherence. A 100 μL aliquot of QuickExtract FFPE Solution (Epicentre Cat# QEF81805, Madison, WI) was added to the slide. Tissue and solution were then scraped into a microcentrifuge tube, heated at 56°C for 1 hour and then 98°C for 2 min, and the DNA was then used for genotyping. The mice were genotyped for SPL status by PCR of embryonic DNA using three primers:

5′CGCTCAGAAGGCTCTGAGTCATGG3′,

5′CATCAAGGAAACCCTGGACTACTG3′, and

5′CCAAGTGTACCTGCTAAGTTCCAG3′ using the following conditions: denaturation, 94 °C for 5 min; amplification, 94 °C for 1 min, 58 °C for 1 min, 72 °C for 1 min (40 cycles); extension, 72 °C for 1 min. The wild type *Sgpl1* gene fragment is approximately 300 bp in length and the null mutant gene fragment is approximately 600 bp in length.

4.4 Immunohistochemistry analysis

For detection of murine SPL protein, we used a polyclonal antibody raised against an amino acid sequence corresponding to the C-terminus of the murine SPL protein. Formalin-fixed and paraffin embedded murine embryonic and placental tissues were deparaffinized and incubated for 30 min in 3% hydrogen peroxide/methanol to quench endogenous peroxidases. Sections were rinsed in PBS and immunostained with anti-(murine) SPL antisera at 1:200 dilution in 0.5% PBS/Ova Albumin at 37°C for 1 h after antigen retrieval with citrate buffer, pH 6.0 in a small autoclave set for 125°C for 2 min; slides were cooled for 1 h at RT before adding secondary antibody. Secondary antibody was biotinylated anti-rabbit (Vector laboratories) diluted 1:1000 in 0.5% PBS/Ova Albumin and incubated for 30 min at RT. Sections were incubated with Elite ABC kit (Vector Laboratories) for 30 min, rinsed in PBS, and detection was performed with DAB (Vector Laboratories) for 2 min, and counterstained in Hematoxylin.

4.5 Microscopy and imaging

Paraffin embedded sections immunostained for the SPL protein were evaluated by a veterinary pathologist (SN) using brightfield microscopy (Olympus BX51) with up to and

including 40x magnification. Images were taken with digital camera (Olympus DP 72) using cellSens Dimension imaging software (Version 1.4) as well as with whole slide images scanned at 40x (Hamamatsu Nanozoomer 2.0). Staining was evaluated for location in cell type, cytoplasmic or nuclear localization, pattern of staining – ie. Vacuolated, stippled, smooth, smudged. Immunostaining was also scored for intensity of stained signal using a semi-quantitative system: 0 = no stain, 1 = minimal, 2 = mild, 3 = moderate, 4 = strong.

Acknowledgments

We are grateful to Nelle Cronen for expert administrative assistance. This work was supported by National Institutes of Health Grants CA77528, GM66954 and CA129438 (JDS).

Abbreviations

CNS	central nervous system
ER	endoplasmic reticulum
S1P	sphingosine-1-phosphate
S1PR	sphingosine-1-phosphate receptor
SPL	sphingosine phosphate lyase

References

Adamson SL, Lu Y, Whiteley KJ, Holmyard D, Hemberger M, Pfarrer C, Cross JC. Interactions between trophoblast cells and the maternal and fetal circulation in the mouse placenta. Dev Biol. 2002; 250:358–373. [PubMed: 12376109]

Allende M, Bektas M, Lee B, Bonifacino E, Kang J, Tuymetova G, Chen W, Saba J, Proia R. Sphingosine-1-phosphate lyase deficiency produces a pro-inflammatory response while impairing neutrophil trafficking. J Biol Chem. 2011; 286:7348–7358. [PubMed: 21173151]

Bandhuvula P, Honbo N, Wang GY, Jin ZQ, Fyrst H, Zhang M, Borowsky AD, Dillard L, Karliner JS, Saba JD. S1P lyase: a novel therapeutic target for ischemia-reperfusion injury of the heart. Am J Physiol Heart Circ Physiol. 2011; 300:H1753–1761. [PubMed: 21335477]

Bektas M, Allende ML, Lee BG, Chen W, Amar MJ, Remaley AT, Saba JD, Proia RL. Sphingosine 1-phosphate lyase deficiency disrupts lipid homeostasis in liver. J Biol Chem. 2010; 285:10880–10889. [PubMed: 20097939]

Borowsky AD, Bandhuvula P, Kumar A, Yoshinaga Y, Nefedov M, Fong LG, Zhang M, Baridon B, Dillard L, de Jong P, Young SG, West DB, Saba JD. Sphingosine-1-phosphate lyase expression in embryonic and adult murine tissues. J Lipid Res. 2012; 53:1920–1931. [PubMed: 22781001]

Duan RD, Nilsson A. Metabolism of sphingolipids in the gut and its relation to inflammation and cancer development. Prog Lipid Res. 2009; 48:62–72. [PubMed: 19027789]

Fang H, Yang Y, Li C, Fu S, Yang Z, Jin G, Wang K, Zhang J, Jin Y. Transcriptome analysis of early organogenesis in human embryos. Dev Cell. 2010; 19:174–184. [PubMed: 20643359]

Hagen N, Hans M, Hartmann D, Swandulla D, van Echten-Deckert G. Sphingosine-1-phosphate links glycosphingolipid metabolism to neurodegeneration via a calpain-mediated mechanism. Cell Death Differ. 2011; 18:1356–1365. [PubMed: 21331079]

Hagen N, Van Veldhoven PP, Proia RL, Park H, Merrill AH Jr, Van Echten-Deckert G. Subcellular origin of sphingosine-1-phosphate is essential for its toxic effect in lyase deficient neurons. J Biol Chem. 2009; 284:11346–11353. [PubMed: 19251691]

Hanel P, Andreani P, Graler M. Erythrocytes store and release sphingosine 1-phosphate in blood. FASEB J. 2007; 21:1202–1209. [PubMed: 17215483]

Johnstone ED, Chan G, Sibley CP, Davidge ST, Lowen B, Guilbert LJ. Sphingosine-1-phosphate inhibition of placental trophoblast differentiation through a G(i)-coupled receptor response. J Lipid Res. 2005; 46:1833–1839. [PubMed: 15995175]

Kumar A, Byun HS, Bittman R, Saba JD. The sphingolipid degradation product trans-2-hexadecenal induces cytoskeletal reorganization and apoptosis in a JNK-dependent manner. Cell Signal. 2011; 23:1144–1152. [PubMed: 21385609]

Kupperman E, An S, Osborne N, Waldron S, Stainier DY. A sphingosine-1-phosphate receptor regulates cell migration during vertebrate heart development. Nature. 2000; 406:192–195. [PubMed: 10910360]

Liu Y, Wada R, Yamashita T, Mi Y, Deng CX, Hobson JP, Rosenfeldt HM, Nava VE, Chae SS, Lee MJ, Liu CH, Hla T, Spiegel S, Proia RL. Edg-1, the G protein-coupled receptor for sphingosine-1-phosphate, is essential for vascular maturation. J Clin Invest. 2000; 106:951–961. [PubMed: 11032855]

Maceyka M, Harikumar KB, Milstien S, Spiegel S. Sphingosine-1-phosphate signaling and its role in disease. Trends Cell Biol. 2012; 22:50–60. [PubMed: 22001186]

Matloubian M, Lo CG, Cinamon G, Lesneski MJ, Xu Y, Brinkmann V, Allende ML, Proia RL, Cyster JG. Lymphocyte egress from thymus and peripheral lymphoid organs is dependent on S1P receptor 1. Nature. 2004; 427:355–360. [PubMed: 14737169]

Mitiku N, Baker JC. Genomic analysis of gastrulation and organogenesis in the mouse. Dev Cell. 2007; 13:897–907. [PubMed: 18061570]

Mizugishi K, Yamashita T, Olivera A, Miller G, Spiegel S, Proia R. Essential role for sphingosine kinases in neural and vascular development. Mol Cell Biol. 2005; 25:11113–11121. [PubMed: 16314531]

Nagy, A.; Gertsenstein, M.; Vintersten, K.; Behringer, RR. Manipulating the mouse embryo: A laboratory manual. 3. Cold Spring Harbor Laboratory; Cold Spring Harbor, NY: 2003.

Nakahara K, Ohkuni A, Kitamura T, Abe K, Naganuma T, Ohno Y, Zoeller RA, Kihara A. The sjogren-larsson syndrome gene encodes a hexadecenal dehydrogenase of the sphingosine 1-phosphate degradation pathway. Mol Cell. 2012; 46:461–471. [PubMed: 22633490]

Olivera A, Eisner C, Kitamura Y, Dillahunt S, Allende L, Tuymetova G, Watford W, Meylan F, Diesner SC, Li L, Schnermann J, Proia RL, Rivera J. Sphingosine kinase 1 and sphingosine-1-phosphate receptor 2 are vital to recovery from anaphylactic shock in mice. J Clin Invest. 2010; 120:1429–1440. [PubMed: 20407207]

Oskouian B, Sooriyakumaran P, Borowsky A, Crans A, Dillard-Telm L, Tam Y, Bandhuvula P, Saba J. Sphingosine-1-phosphate lyase potentiates apoptosis via p53- and p38-dependent pathways and is downregulated in colon cancer. Proc Natl Acad Sci U S A. 2006; 103:17384–17389. [PubMed: 17090686]

Peng X, Hassoun PM, Sammani S, McVerry BJ, Burne MJ, Rabb H, Pearse D, Tuder RM, Garcia JG. Protective effects of sphingosine 1-phosphate in murine endotoxin-induced inflammatory lung injury. Am J Respir Crit Care Med. 2004; 169:1245–1251. [PubMed: 15020292]

Poulsen RR, McClaskey CM, Rivkees SA, Wendler CC. The Sphingosine-1-phospate receptor 1 mediates S1P action during cardiac development. BMC Dev Biol. 2011; 11:37. [PubMed: 21668976]

Schmahl J, Raymond CS, Soriano P. PDGF signaling specificity is mediated through multiple immediate early genes. Nat Genet. 2007; 39:52–60. [PubMed: 17143286]

Schwab S, Pereira J, Matloubian M, Xu Y, Huang Y, Cyster J. Lymphocyte sequestration through S1P lyase inhibition an disruption of S1P gradients. Science. 2005; 309:1735–1739. [PubMed: 16151014]

Serra M, Saba JD. Sphingosine 1-phosphate lyase, a key regulator of sphingosine 1-phosphate signaling and function. Adv Enzyme Regul. 2010; 50:349–362. [PubMed: 19914275]

Siow D, Anderson C, Berdyshev E, Skobeleva A, Pitson S, Wattenberg B. Intracellular localization of sphingosine kinase 1 alters access to substrate pools but does not affect the degradative fate of sphingosine-1-phosphate. J Lipid Res. 2010; 51:2546–2559. [PubMed: 20386061]

Stein JV, Nombela-Arrieta C. Chemokine control of lymphocyte trafficking: a general overview. Immunology. 2005; 116:1–12. [PubMed: 16108812]

Upadhyaya P, Kumar A, Byun HS, Bittman R, Saba JD, Hecht SS. The sphingolipid degradation product trans-2-hexadecenal forms adducts with DNA. Biochem Biophys Res Commun. 2012; 424:18–21. [PubMed: 22727907]

Van Veldhoven PP, Gijsbers S, Mannaerts GP, Vermeesch JR, Brys V. Human sphingosine-1-phosphate lyase: cDNA cloning, functional expression studies and mapping to chromosome 10q22. Biochim Biophys Acta. 2000; 1487:128–134. [PubMed: 11018465]

Vogel P, Donoviel MS, Read R, Hansen GM, Hazlewood J, Anderson SJ, Sun W, Swaffield J, Oravecz T. Incomplete inhibition of sphingosine 1-phosphate lyase modulates immune system function yet prevents early lethality and non-lymphoid lesions. PLoS One. 2009; 4:e4112. [PubMed: 19119317]

Ward, J.; Mann, P.; Morishima, H.; Frith, C. Thymus, Spleen and Lymph Nodes. In: Maronpot, R., editor. Pathology of the Mouse. Cache River Press; St. Louis, MO: 1999. p. 333-338.

Watson ED, Cross JC. Development of structures and transport functions in the mouse placenta. Physiology (Bethesda). 2005; 20:180–193. [PubMed: 15888575]

Weber C, Krueger A, Munk A, Bode C, Van Veldhoven PP, Graler MH. Discontinued postnatal thymocyte development in sphingosine 1-phosphate-lyase-deficient mice. J Immunol. 2009; 183:4292–4301. [PubMed: 19748984]

Yamamoto Y, Olson DM, van Bennekom M, Brindley DN, Hemmings DG. Increased expression of enzymes for sphingosine 1-phosphate turnover and signaling in human decidua during late pregnancy. Biol Reprod. 2010; 82:628–635. [PubMed: 20007411]

Zhou J, Saba J. Identification of the first mammalian sphingosine phosphate lyase gene and its functional expression in yeast. Biochem Biophys Res Commun. 1998; 242:502–507. [PubMed: 9464245]

Highlights

1. SPL is expressed in murine placenta, with highest levels in spongiotrophoblast layer
2. SPL expression in maternal sinusoids suggests a role in maternal-fetal exchange
3. Intensity of SPL expression changes dynamically over time during murine development
4. Embryonic SPL expression pattern is consistent with SPL mutant congenital phenotypes
5. Expression of mSPL in key embryonic structures predicts its adult expression pattern

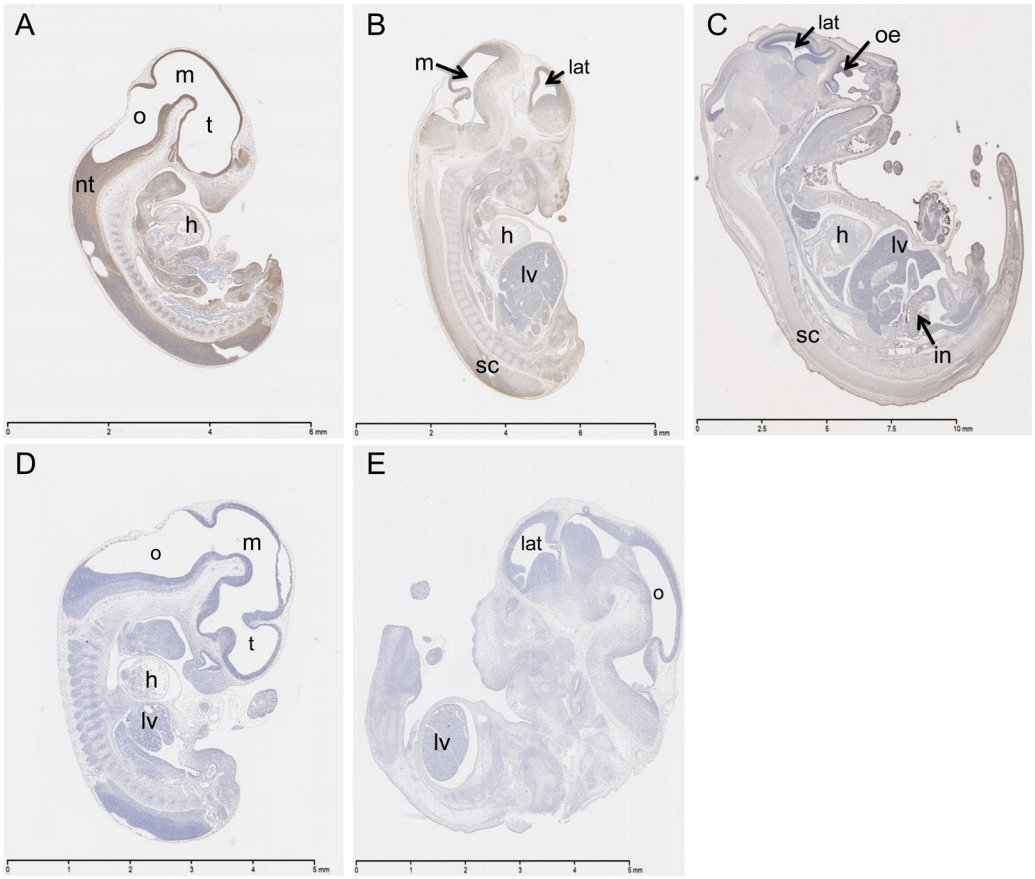

Fig 1.

Sagittal embryo sections. Immunostained for SPL protein, counterstained with hematoxylin. A. Wild type E12 embryo with ubiquitous moderate to strong staining throughout all organ systems. Scale bar 6mm. B. Wild type E15 embryo revealed mild to moderate ubiquitous staining throughout all organs. Scale bar 8 mm. C. Wild type E18 with a range of moderate to strong, more organ specific immunopositivity. Scale bar 10 mm. D. SPL knockout E12 embryo negative control. Scale bar 5 mm E. SPL knockout E15 embryo negative control. Scale bar 5 mm. h – heart, in – intestine, lat – lateral ventricle, lv – liver, m- mesencephalon, nt – neural tube, o – fourth ventricle, oe – olfactory epithelium, sc – spinal cord, t- telencephalon.

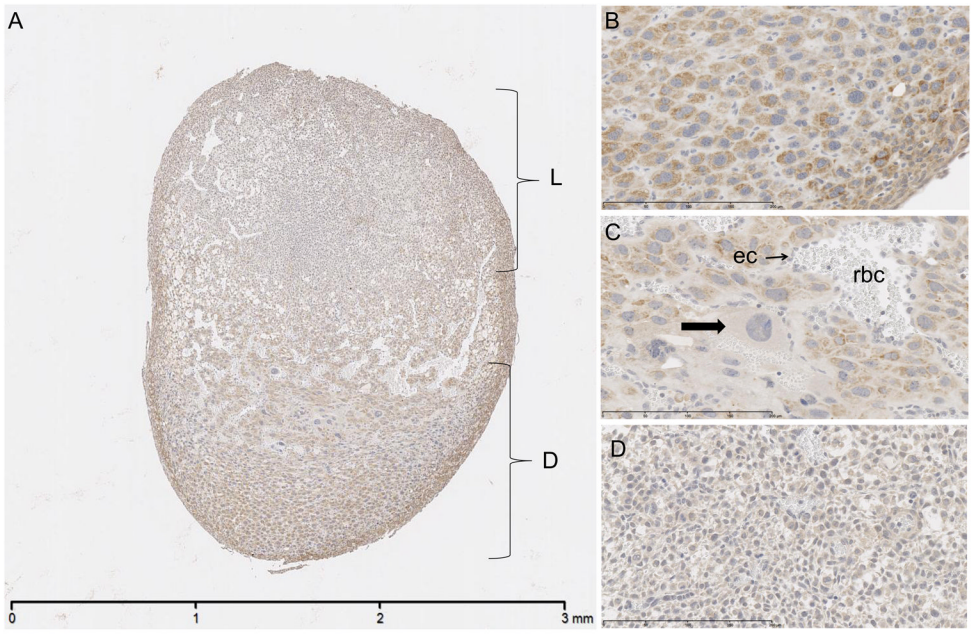

Fig 2.

E8 placenta. Immunostained for SPL protein, counterstained with hematoxylin. A. Decidua (D) with moderate to strong cytoplasmic signal and weaker signal in labyrinth (L). Scale bar 3 mm. B. Decidual cells with minimal to mild cytoplasmic signal. Scale bar 200 um. C. Giant cell trophoblasts (arrow) with absent to minimal signal. ec – endothelial cell, rbc – red blood cells. Scale bar 200 um. D. Labyrinth spongiotrophoblasts with minimal to mild signal. Scale bar 200 um.

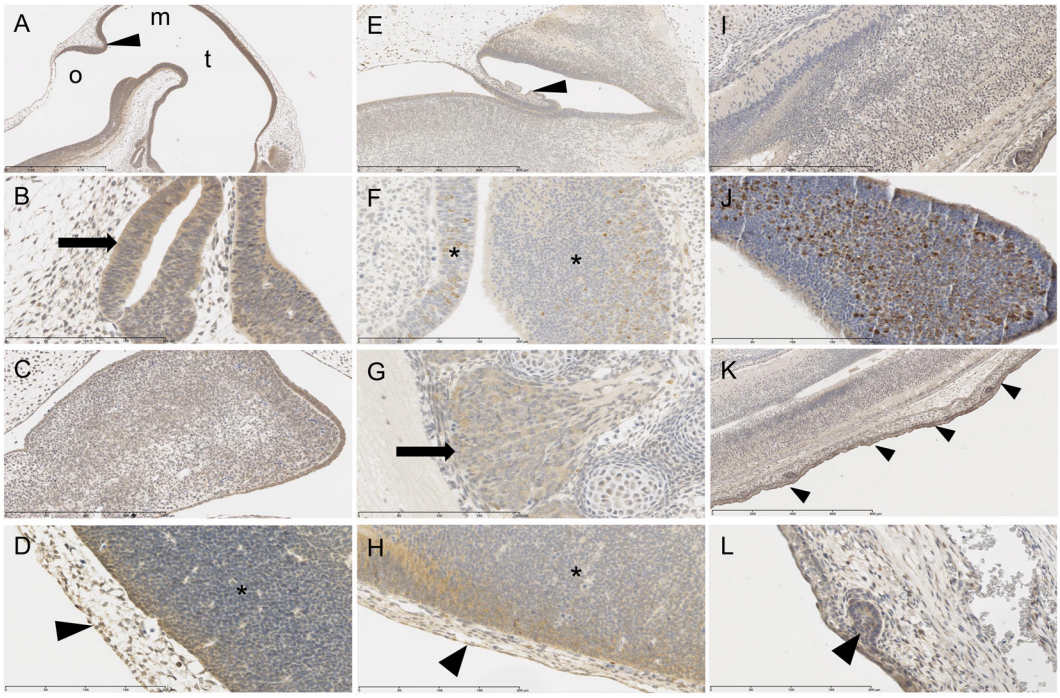

Fig 3.

Ectoderm organ systems immunostained for SPL protein with positive cytoplasmic signal, counterstained with hematoxylin. E12: A. cells lining the third ventricle (t) fourth ventricle (o), mesancephalic vesicle (m) and cerebellar primordium (arrowhead). Scale bar 1 mm. B. Rathke's pouch (arrow). Scale bar 200 um. C. mandibular component of the first brachial arch. Scale bar 400 um. D. epidermis (arrowhead) and neural tube (*). 200 um. E15: E. choroid plexus (arrowhead). Scale bar 800 um. F. olfactory epithelium (*). Scale bar 200 um. G. dorsal root ganglion (arrow). Scale bar 200 um. H. epidermis (arrowhead) and neural tube (*). Scale bar 200 um. E18: I. spinal cord. Scale bar 400 um. J. olfactory epithelium. Scale bar 200 um. K. epidermis (arrowheads). Scale bar 800 um. L. developing pilosebaceous unit (arrowhead). Scale bar 200 um.

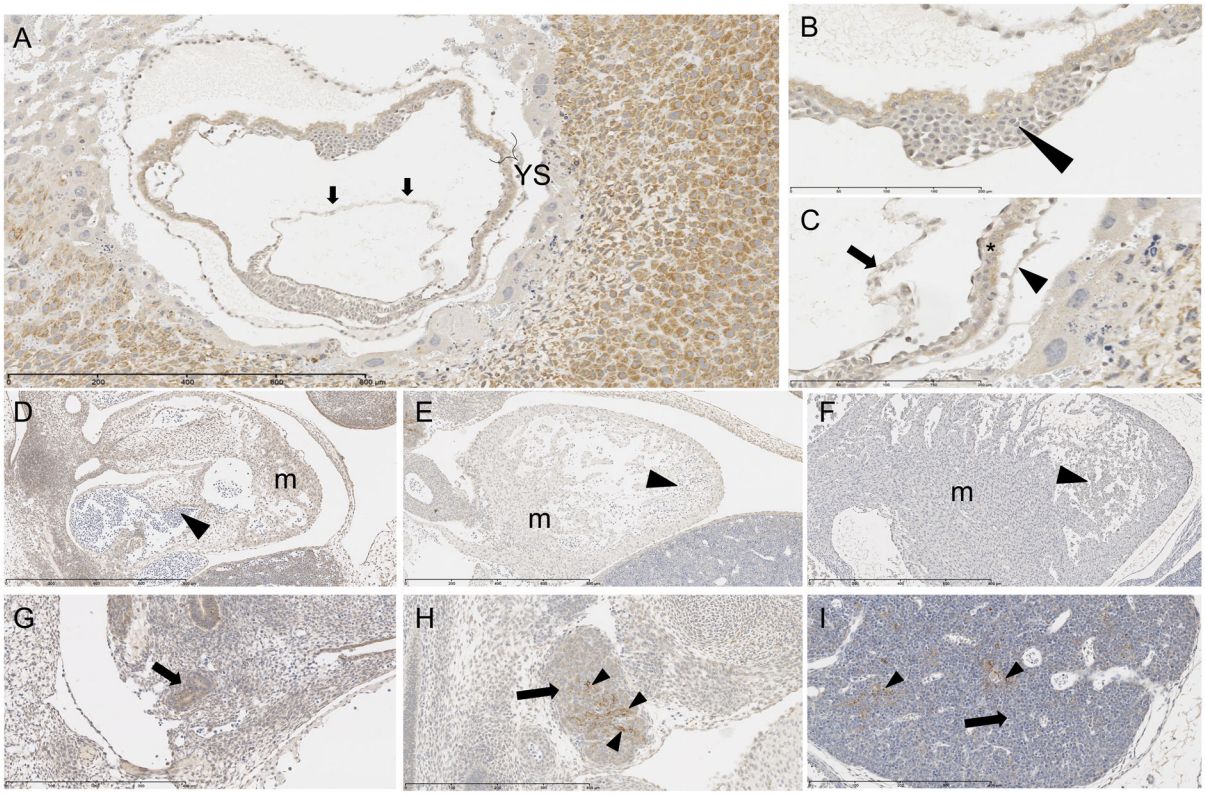

Fig 4.

Mesoderm organ systems immunostained for SPL protein with positive cytoplasmic signal, counterstained with hematoxylin. E8: A. Amnion (arrows) and yolk sac (YS) with moderate positive signal. Scale bar 800 um. B. Blood island (arrowhead) of yolk sac with positive endothelial lining and positive fetal precursor red blood cells. Scale bar 200 um. C. Amnion (arrow) parietal (arrowhead) and visceral (*) layers of yolk sac with positive signal. Scale bar 200 um. E12: D. Moderately positive signal in myocardium (m), negative in red blood cells (arrowhead). Scale bar 800 um. E15: E. Mild positive signal in myocardium (m), negative in red blood cells (arrowhead). Scale bar 800 um. E18: F. Negative signal in myocardium (m) and red blood cells (arrowhead). Scale bar 800 um. E12: G. Positive signal in primordial thymus (derivative of third brachial arch) (arrow). Scale bar 400 um. E15: H. Minimal scattered positive signal in lymphocytes (arrow) of thymus, but had mild to strong patchy positive signal in thymic epithelial (reticular) cytoplasm (arrowheads), which are derived from endoderm. Scale bar 400 um. E18: I. Negative signal in lymphocytes (arrow) of thymus, but scattered mild to strong positive signal in thymic epithelial (reticular) cytoplasm (arrowheads), which are derived from endoderm. Scale bar 400 um.

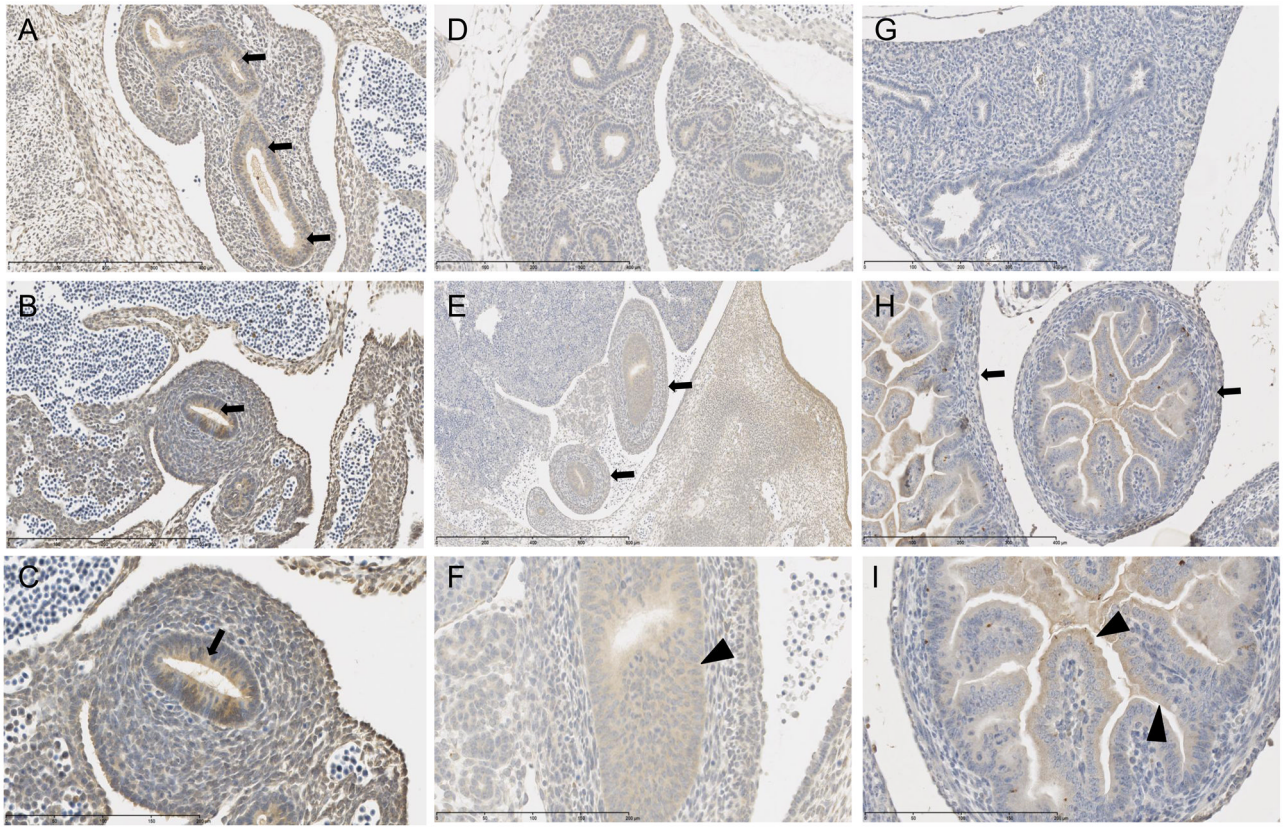

Fig 5.

Endoderm organ systems immunostained for SPL protein with positive cytoplasmic signal, counterstained with hematoxylin. E12: A. Lung bud with positive signal in cytoplasm of primordial lung epithelium (arrows). Scale bar 400 um. B. Intestinal epithelium with positive cytoplasmic signal (arrow). Scale bar 400 um. C. Higher magnification of B showing signal near apical portion of epithelial cells. Scale bar 200 um. E15: D. Lungs with moderate to strong cytoplasmic signal throughout the tissue. Scale bar 400 um. E. Developing intestinal tract with minimal to mild cytoplasmic staining in future submucosa, muscularis mucosa and serosa (arrows). Scale bar 800 um. F. Higher magnification of E reveals mild cytoplasmic staining in mucosal cells of intestinal tract (arrowhead). Scale bar 200 um. E18: G. Absence of immunohistochemical signal in lung. Scale bar 400 um. H. Minimal cytoplasmic signal in developing submucosa, muscularis mucosa and serosa (arrows). Scale bar 400 um. I. Mild cytoplasmic signal in apical cytoplasm of enterocytes (arrowheads). Scale bar 200 um.